

# Fully Generalized Optical Spatial Modulation

1<sup>st</sup> Yinan Zhao

*School of Microelectronics and Communication Engineering  
Chongqing University  
Chongqing, China  
20211201011@cqu.edu.cn*

2<sup>nd</sup> Chen Chen

*School of Microelectronics and Communication Engineering  
Chongqing University  
Chongqing, China  
c.chen@cqu.edu.cn*

3<sup>rd</sup> Lin Zeng

*School of Microelectronics and Communication Engineering  
Chongqing University  
Chongqing, China  
202012021008@cqu.edu.cn*

4<sup>th</sup> Min Liu

*School of Microelectronics and Communication Engineering  
Chongqing University  
Chongqing, China  
liumin@cqu.edu.cn*

**Abstract**—In this paper, we propose and investigate two fully generalized optical spatial modulation (FGOSM) schemes for multiple-input multiple-output (MIMO-OWC) systems, including one-dimensional FGOSM (1D-FGOSM) and two-dimensional FGOSM (2D-FGOSM). Our proposed FGOSM schemes can significantly improve the spectral efficiency of the MIMO-OWC system compared with conventional optical spatial modulation (OSM) and generalized optical spatial modulation (GOSM) schemes. Simulation results show that, for a spectral efficiency of 6 bits/s/Hz, remarkable signal-to-noise ratio (SNR) gains of 4.5 and 8.4 dB are achieved by 1D-FGOSM and 2D-FGOSM in comparison to GOSM, respectively.

**Index Terms**—Optical wireless communication, multiple-input multiple-output, generalized optical spatial modulation.

## I. INTRODUCTION

CURRENTLY, wireless access is primarily achieved via the use of the radio frequency (RF) spectrum. However, recent forecasts indicate that there will not be enough RF spectrum available for the ever-increasing wireless access by 2035 [1]. Optical Wireless Communication (OWC) has been envisaged as a promising complementary technology to ease the RF spectrum crunch [2]. However, despite the various benefits of OWC systems, the available modulation bandwidth of commercial off-the-shelf optical components is limited, especially the white light-emitting diode (LED)s [3]. Since white LED-based OWC systems usually have a limited -3dB bandwidth of only a few MHz [4], the use of multiple-input multiple-output (MIMO) transmission can be one potential way to enhance the capacity of OWC systems [5].

As a digitized MIMO scheme, optical spatial modulation (OSM) has been widely applied in MIMO-OWC systems, due to its inherent advantages such as negligible inter-channel interference (ICI), high power efficiency and low transceiver complexity [6]–[8]. Nevertheless, it is very difficult for OSM systems to achieve a relatively high spectral efficiency [9]. Recently, GOSM schemes have been proposed to increase

This work was supported in part by the National Natural Science Foundation of China under Grant 62271091 and 61901065, and in part by the Natural Science Foundation of Chongqing under Grant cstc2021jcyj-msxmX0480.

the spectral efficiency of MIMO-OWC systems, which can activate more than one LED to transmit the same signal at each time slot [10]. Moreover, the GOSM mapping can be performed jointly among adjacent two time slots, i.e., a time block, so as to further enhance the achievable spectral efficiency [11]. However, in the current existing GOSM systems, a fixed number of LEDs are selected and activated at each time slot or time block, and hence the potential benefit of activating a variable number of LEDs has not been explored.

In this paper, we propose two fully generalized optical spatial modulation (FGOSM) schemes, i.e., one-dimensional FGOSM (1D-FGOSM) and two-dimensional FGOSM (2D-FGOSM), for MIMO-OWC systems. In 1D-FGOSM, the number of activated LEDs at each time slot is variable. Moreover, in 2D-FGOSM, two successive time slots are grouped as one time block and the number of activated LEDs at each time block is also variable. Compared with conventional OSM and GOSM schemes, the proposed FGOSM schemes can substantially enhance the spectral efficiency of MIMO-OWC systems. Simulation results demonstrate the feasibility and superiority of the proposed FGOSM schemes in a typical MIMO-OWC system.

## II. SYSTEM MODEL

We consider a typical MIMO-OWC system equipped with  $N_t$  LEDs and  $N_r$  photo-detectors (PDs), where the LEDs are spaced equally across the ceiling and the PDs are located over the receiving plane of the room. At the receiver side, the received signal vector can be expressed by

$$\mathbf{y} = \mathbf{Hx} + \mathbf{n}, \quad (1)$$

where  $\mathbf{x}$  is the transmitted signal vector,  $\mathbf{H}$  is the  $N_r \times N_t$  MIMO channel matrix, and  $\mathbf{n}$  is the additive noise vector.

Assuming only line-of-sight (LOS) transmission, the channel gain between the  $t$ -th LED and the  $r$ -th PD can be calculated by [12]

$$h_{rt} = \frac{(m+1)\rho A}{2\pi d_{rt}^2} \cos^m(\varphi) T_s(\theta) g(\theta) \cos(\theta), \quad (2)$$

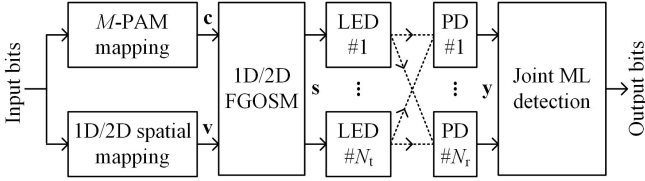


Fig. 1. Schematic diagram of the proposed 1D/2D-FGOSM system.

where  $m = -\ln 2 / \ln(\cos(\Psi))$  is the Lambertian emission order and  $\Psi$  is the semi-angle at half power of the LED;  $\rho$  and  $A$  represent the responsivity and the active area of the PD, respectively; the distance between the  $t$ -th LED and the  $r$ -th PD is denoted by  $d_{rt}$ . Furthermore,  $\varphi$  and  $\theta$  represent the angles of emission and incidence, respectively.  $T_s(\theta)$  denotes the gain of optical filter; the gain of optical lens is represented by  $g(\theta) = \frac{n^2}{\sin^2 \Phi}$  with  $\Phi$  and  $n$  being the refractive index and the half-angle field-of view (FOV) of the optical lens, respectively.

In addition, the additive noise in typical OWC systems usually includes the thermal noise, shot noise and possibly excess noise, and it can be reasonably modeled as a real-valued additive white Gaussian noise (AWGN) with zero mean and variance  $P_n$ . The variance, i.e., noise power, can be given by  $P_n = N_0 B$ , where  $N_0$  denotes the power spectral density (PSD) and  $B$  is the signal bandwidth.

### III. PROPOSED FGOSM SCHEMES FOR MIMO-OWC

In this section, we introduce the principle of the proposed FGOSM schemes for MIMO-OWC systems, where the  $M$ -ary pulse amplitude modulation ( $M$ -PAM) is considered as the modulation format due to its low complexity [11]. Fig. 1 depicts the schematic diagram of the proposed 1D/2D-FGOSM system, where the input bits are first divided into two streams: one is mapped into a  $M$ -PAM symbol vector  $c$ ; the other is mapped into a 1D/2D spatial index vector  $v$ . Subsequently, the 1D/2D-FGOSM mapping is performed to generate the transmitted signal vector  $s$  at the transmitter side. After propagation through the spatial channel, the optical signal is detected by a PD array and the joint maximum-likelihood (ML) detection is adopted for signal detection so as to generate the final output bits.

#### A. 1D-FGOSM

The principle of 1D-FGOSM spatial mapping is illustrated in Fig. 2(a), where we assume there are totally four LEDs in the MIMO-OWC system, i.e.,  $N_t = 4$ . As we can see, the number of activated LEDs can be variable at different time slots and the feasible number of activated LEDs can be one, two, three and four. Assuming  $i$  out of  $N_t$  LEDs are selected and activated to transmit the same  $M$ -PAM symbol at a specific time slot, the number of possible LED activation patterns is then given by  $C(N_t, i)$ , where  $C(\cdot, \cdot)$  denotes the binomial coefficient. As a result, for  $i \in \{1, 2, \dots, N_t\}$ , the total number of possible LED activation patterns is calculated by  $\sum_{i=1}^{N_t} C(N_t, i)$ . Therefore, the achievable spectral

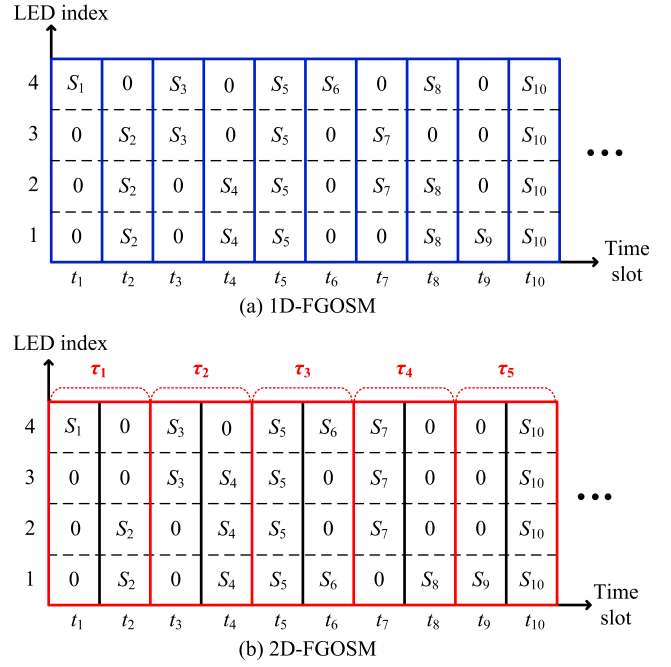


Fig. 2. Principle of the proposed FGOSM Schemes: (a) 1D-FGOSM and (b) 2D-FGOSM.

efficiency of the MIMO-OWC system applying the proposed 1D-FGOSM scheme with  $M$ -PAM can be obtained by

$$R_{\text{FGOSM}}^{\text{1D}} = \left\lfloor \log_2 \left( M \sum_{i=1}^{N_t} C(N_t, i) \right) \right\rfloor, \quad (3)$$

where  $\lfloor \cdot \rfloor$  denotes the floor operation.

#### B. 2D-FGOSM

It can be observed from Fig. 2(a) that the spatial mapping in 1D-FGOSM is executed with respect to each individual time slot. In contrast, in the proposed 2D-FGOSM, the spatial mapping is performed jointly among two successive time slots. Fig. 2(b) shows the principle of 2D-FGOSM spatial mapping, where two consecutive time slots are grouped into one time block, and two  $M$ -PAM constellations, i.e.,  $M_1$ -PAM and  $M_2$ -PAM, can be transmitted at the first and second time slots of the time block, respectively. Similarly, the number of activated LEDs at each time slot of the time block is also variable in 2D-FGOSM. Letting  $i \in \{1, 2, \dots, N_t\}$  and  $j \in \{1, 2, \dots, N_t\}$  respectively denote the numbers of LEDs activated to transmit the  $M_1$ -PAM and  $M_2$ -PAM symbols at the first and second time slots of the time block, the total number of possible LED activation patterns within each time block can be expressed by  $\sum_{i=1}^{N_t} C(N_t, i) \sum_{j=1}^{N_t} C(N_t, j)$ . Consequently, the achievable spectral efficiency of the MIMO-OWC system employing the proposed 2D-FGOSM scheme can be calculated by

$$R_{\text{FGOSM}}^{\text{2D}} = \frac{1}{2} \left\lfloor \log_2 \left( M_1 M_2 \sum_{i=1}^{N_t} C(N_t, i) \sum_{j=1}^{N_t} C(N_t, j) \right) \right\rfloor. \quad (4)$$

TABLE I  
SIMULATION PARAMETERS

Parameter	Value
Room dimension	$4 \text{ m} \times 4 \text{ m} \times 3 \text{ m}$
LED spacing	2 m
APD spacing	15 cm
Semi-angle at half power of LED	$65^\circ$
Gain of optical filter	0.9
Refractive index of optical lens	1.5
Half-angle FOV of optical lens	$65^\circ$
Responsivity of APD	15 A/W
Height of receiving plane	0.85 m
Active area of APD	19.6 mm
Noise PSD	$10^{-22} \text{ A}^2/\text{Hz}$
Modulation bandwidth	20MHz
Number of LEDs	4
Number of APDs	4
Receiver location	(1.5 m, 1.5 m, 0.85 m)

For the purpose of comparison, the spectral efficiencies of the MIMO-OWC system using conventional OSM and GOSM with a fixed number of  $N_a$  activated LEDs are given as follows:

$$R_{\text{OSM}} = \left\lfloor \log_2 \left( M \sum_{i=1}^{N_t} C(N_t, 1) \right) \right\rfloor, \quad (5)$$

$$R_{\text{GOSM}} = \left\lfloor \log_2 \left( M \sum_{i=1}^{N_t} C(N_t, N_a) \right) \right\rfloor. \quad (6)$$

By comparing Eqs. (5) and (6) with Eqs. (3) and (4), we can see that the proposed FGOSM schemes can efficiently improve the achievable spectral efficiency of the MIMO-OWC system when compared with conventional OSM and GOSM.

#### IV. SIMULATION RESULTS

In this section, we conduct numerical simulations to investigate the performance of the MIMO-OWC system using the proposed FGOSM schemes. Particularly, we configure a  $4 \times 4$  MIMO-OWC system in a typical indoor  $4 \text{ m} \times 4 \text{ m} \times 3 \text{ m}$  room, where the four LEDs are mounted on the ceiling and the user equipped with a  $2 \times 2$  avalanche PD (APD) array is located at the location (1.5 m, 1.5 m, 0.85 m) over the receiving plane. For performance comparison, conventional OSM and GOSM with two active LEDs selected out of four LEDs are adopted as the benchmark schemes. The key parameters of the simulation setup are listed in Table I.

We first evaluate and compare the spectral efficiency of different schemes in the  $4 \times 4$  MIMO-OWC system. Fig. 3(a) depicts the spectral efficiency versus  $\log_2 M$  for OSM, GOSM and 1D-FGOSM. As we can observe, the same spectral efficiency can be achieved by OSM and GOSM schemes, while the spectral efficiency of the proposed 1D-FGOSM is always 1 bit/s/Hz higher than that of OSM and GOSM for different  $\log_2 M$  values. Moreover, the spectral efficiency versus  $\log_2 M_1$  and  $\log_2 M_2$  for 2D-FGOSM is depicted in Fig. 3(b). It can be seen that the spectral efficiency of 2D-FGOSM is jointly determined by  $\log_2 M_1$  and  $\log_2 M_2$ , and a significant

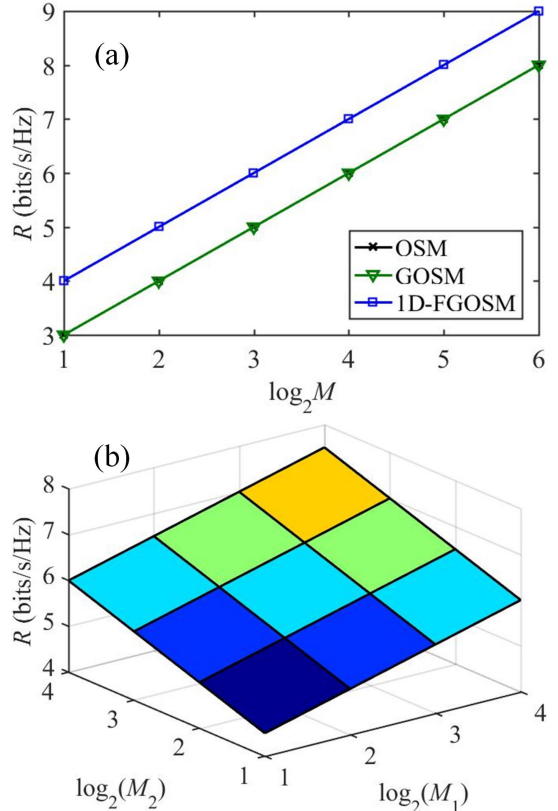


Fig. 3. (a) Spectral efficiency vs.  $\log_2 M$  for OSM, GOSM and 1D-FGOSM; (b) spectral efficiency vs.  $\log_2 M_1$  and  $\log_2 M_2$  for 2D-FGOSM.

spectral efficiency enhancement can be obtained over OSM, GOSM and 1D-FGOSM when we set  $M_1 = M_2 = M$ .

In the next, we investigate and compare the bit error rate (BER) performance of different schemes in the  $4 \times 4$  MIMO-OWC system, where we consider three spectral efficiencies of 5, 6, and 7 bit/s/Hz. To reach a target spectral efficiency, the required  $M$  values for OSM, GOSM and 1D-FGOSM can be directly obtained according to Fig. 3(a), while there are more than one combination of  $\{M_1, M_2\}$  for 2D-FGOSM as shown in Fig. 3(b). Here, the combinations of  $\{M_1, M_2\}$  for 2D-FGOSM to achieve the spectral efficiencies of 5, 6, and 7 bit/s/Hz are selected to be  $\{2, 4\}$ ,  $\{4, 8\}$  and  $\{8, 16\}$ , respectively.

Figs. 4(a), (b) and (c) shows the BER versus average received SNR for the  $4 \times 4$  MIMO-OWC system using different schemes achieving spectral efficiencies of 5, 6, and 7 bit/s/Hz, respectively. For a spectral efficiency of 5 bits/s/Hz, as shown in Fig. 4(a), OSM and GOSM obtain comparable BER performance, both requiring an average received SNR of about 36.2 dB to reach the BER threshold of  $3.8 \times 10^{-3}$ . In contrast, the required average received SNRs for 1D-FGOSM and 2D-FGOSM to reach  $\text{BER} = 3.8 \times 10^{-3}$  are 32.2 and 31.2 dB, respectively. Hence, a 4 dB SNR is achieved by 1D-FGOSM in comparison to conventional OSM and GOSM, while 2D-FGOSM further outperforms 1D-FGOSM by an SNR gain of 1 dB. When the spectral efficiency is increased

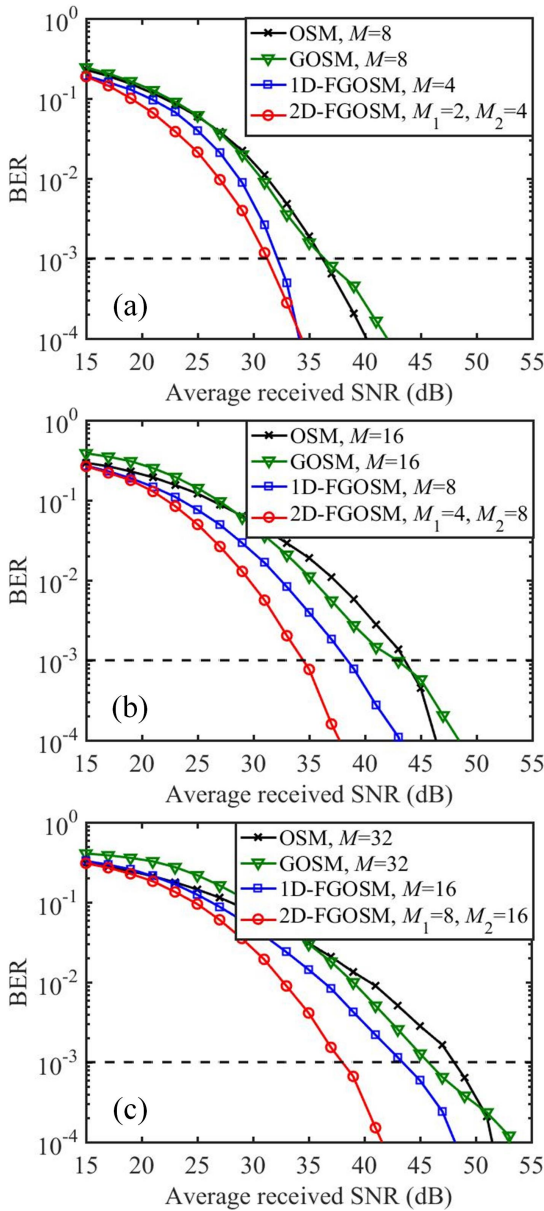


Fig. 4. BER vs. average received SNR for a spectral efficiency of (a) 5 bits/s/Hz, (b) 6 bits/s/Hz and (c) 7 bits/s/Hz.

to 6 and 7 bits/s/Hz, as can be seen from Figs. 4(b) and (c), GOSM gradually outperforms OSM, and meanwhile the performance gain of 2D-FGOSM over 1D-FGOSM becomes quite significant. More specifically, for a spectral efficiency of 6 bits/s/Hz, 1D-FGOSM and 2D-FGOSM outperform GOSM by SNR gains of 4.5 and 8.4 dB, respectively.

## V. CONCLUSION

In this paper, we have proposed and evaluated two FGOSM schemes for bandlimited MIMO-OWC systems. Compared with conventional OSM and GOSM, substantial spectral efficiency improvement can be obtained by the proposed FGOSM schemes via varying the number of activated LEDs and joint spatial mapping over two successive time slots. Our simulation

results show that both the proposed 1D-FGOSM and 2D-FGOSM schemes perform better than conventional OSM and GOSM, while 2D-FGOSM outperforms 1D-FGOSM when the target spectral efficiency is relatively large. Therefore, the proposed FGOSM schemes can be promising candidates for practical bandlimited MIMO-OWC systems.

## REFERENCES

- [1] I. Tavakkolnia, L. K. Jagadamma, R. Bian, P. P. Manousiadis, S. Videv, G. A. Turnbull, I. D. Samuel, and H. Haas, "Organic photovoltaics for simultaneous energy harvesting and high-speed MIMO optical wireless communications," *Light: Science & Applications*, vol. 10, no. 1, pp. 1–11, 2021.
- [2] C.-H. Yeh, L.-Y. Wei, and C.-W. Chow, "Using a single VCSEL source employing OFDM downstream signal and remodulated OOK upstream signal for bi-directional visible light communications," *Scientific Reports*, vol. 7, no. 1, pp. 1–6, 2017.
- [3] S. Rajagopal, R. D. Roberts, and S.-K. Lim, "IEEE 802.15. 7 visible light communication: modulation schemes and dimming support," *IEEE Communications Magazine*, vol. 50, no. 3, pp. 72–82, 2012.
- [4] A. Ren, H. Wang, W. Zhang, J. Wu, Z. Wang, R. V. Penty, and I. H. White, "Emerging light-emitting diodes for next-generation data communications," *Nature Electronics*, vol. 4, no. 8, pp. 559–572, 2021.
- [5] T. Fath and H. Haas, "Performance comparison of MIMO techniques for optical wireless communications in indoor environments," *IEEE Transactions on Communications*, vol. 61, no. 2, pp. 733–742, 2012.
- [6] R. Mesleh, R. Mehmood, H. Elgala, and H. Haas, "Indoor MIMO optical wireless communication using spatial modulation," in *2010 IEEE International Conference on Communications*, 2010, pp. 1–5.
- [7] R. Mesleh, H. Elgala, and H. Haas, "Optical spatial modulation," *Journal of Optical Communications and Networking*, vol. 3, no. 3, pp. 234–244, 2011.
- [8] C. Chen, X. Zhong, S. Fu, X. Jian, M. Liu, X. Deng, and H. Fu, "Enhanced OFDM-based optical spatial modulation," in *ICC 2021-IEEE International Conference on Communications*, 2021, pp. 1–6.
- [9] C. Chen, X. Zhong, S. Fu, X. Jian, M. Liu, H. Yang, A. Alphones, and H. Fu, "OFDM-based generalized optical MIMO," *Journal of Lightwave Technology*, vol. 39, no. 19, pp. 6063–6075, 2021.
- [10] C. R. Kumar and R. Jeyachitra, "Power efficient generalized spatial modulation MIMO for indoor visible light communications," *IEEE Photonics Technology Letters*, vol. 29, no. 11, pp. 921–924, 2017.
- [11] C. Chen, L. Zeng, X. Zhong, S. Fu, Z. Zeng, M. Liu, and H. Haas, "2D generalized optical spatial modulation for MIMO-OWC systems," *IEEE Photonics Journal*, vol. 14, no. 4, pp. 1–6, 2022.
- [12] T. Komine and M. Nakagawa, "Fundamental analysis for visible-light communication system using LED lights," *IEEE Trans. Consum. Electron.*, vol. 50, no. 1, pp. 100–107, 2004.